6-35-618
7

CLIMATE RELATED MEASUREMENTS WITH THE NEW 1.6 μm AVHRR CHANNEL

C. G. Justus, Principal Investigator

School of Earth and Atmospheric Sciences

Georgia Institute of Technology

Atlanta, GA 30332-0340

November, 1993

FINAL PERFORMANCE REPORT

Report Period: September 1, 1991 - August 31, 1993

PREPARED FOR THE

UNITED STATES DEPARTMENT OF COMMERCE

NATIONAL OCEANIC AND ATMOSPHERIC ADMINISTRATION

Under Grant No. NA16RC0448-01

Dr. Arnold Gruber, Technical Monitor

Georgia Tech Project G-35-618/G-35-676

Abstract

An analysis is performed with simulated AVHRR data including the 1.6 μm channel (3A) that will become available on NOAA-K to show that the AVHRR "tasseled cap" transform variables are effective measures of soil moisture and vegetation moisture. Observed soil moisture and vegetation moisture data from the First International Satellite Land Surface Climatology Project (ISLSCP) Field Experiment (FIFE) are examined and shown to verify that the AVHRR tasseled cap transform variables (as represented by Landsat Thematic Mapper surrogate data) provide effective measures of soil moisture change and vegetation moisture content. It is recommended that tasseled cap transform variables be produced from AVHRR data including the new 1.6 μm channel and it id suggested that these quantities will provide useful adjuncts to soil and vegetation moisture determined from microwave sensors. Additionally, it is suggested that the tasseled cap transform AVHRR variables will be useful for other applications such as snow/cloud discrimination, discrimination of water-phase clouds from ice-phase clouds and in the determination of optical properties of cirrus clouds and atmospheric aerosols.

Introduction

Beginning with NOAA-K, the AVHRR instrument is to have a new 1.6 μm channel. This new channel, designated 3A, will be switched over from the normal 3.7 μm (channel 3) during the daylight portion of the orbit. The primary purpose of the new channel 3A is to improve the ability to distinguish between snow and clouds (especially low clouds that have about the same brightness temperature as the surface; see Figures 9-11 of Justus and Paris, 1986).

The purpose of this study is to examine the potential climate-related measurements that might be made on a global scale using the AVHRR data from the new 1.6 μm channel 3A, especially the measurement of soil moisture and vegetation moisture parameters. In addition to these vegetation-moisture and soil-moisture applications documented here, experience with Landsat TM multispectral analysis has shown that the availability of a 1.6 μm channel (such as Band 5 of TM) can be of great value in the quantitative analysis of vegetation status (Tucker, 1978; Perry and Lautenschlager, 1984; Ehrlich et al, 1993) and in the monitoring of fire damage to tropical forests (Pereira and Setzer, 1993). Theoretical spectral model studies have also shown that multispectral analysis including a 1.6 μm channel on AVHRR will have value in the measurement of cirrus clouds (Masuda and Takashima, 1990), in allowing the discrimination between water-phase clouds and ice-phase clouds (Pilewskie and Twomey, 1986), and in the refinement of the determination of aerosol optical properties (Justus and Paris, 1987). The addition of the 1.6 μm channel on AVHRR is therefore expected to provide significant improvement in the global-scale analysis of a variety of climate-related parameters during the period until even more advanced spectral sensors such as MODIS become available (Townsend et al., 1991).

Study Results

The basis for the application of a 1.6 μm sensor wavelength in the determination of soil moisture and vegetation moisture, as well as in snow/cloud discrimination and water-phase-cloud/ice-phase-cloud discrimination, is illustrated in Figures 1 and 2. These figures show spectral reflectance curves taken from Bowker et al. (1985). These figures illustrate that the spectral absorption feature caused by water, normally centered at 1.4 μm if the water is in the vapor phase, is spectrally shifted to 1.5 μm or longer wavelengths if the water is in more solid phase such as snow, ice or moisture content in soil or vegetation.

Normal vegetation index values are based on the difference between reflectance in the visible (0.5-0.7 μm: AVHRR channel 1) and near-IR (0.7-1.0 μm: AVHRR channel 2). Information about the spectral reflectance near 1.5 μm (such as provided by the channel 3A AVHRR at 1.6 μm) is much more sensitive to moisture than the conventional channel 1-channel 2 vegetation index analysis.

Multispectral analysis capabilities can be put on a much more quantitative basis by using the spectral reflectances of Bowker et al. (1985) in a spectral radiative transfer model to simulate the response of the AVHRR sensor in each of its spectral channels, under a variety of observing conditions. For clear-atmosphere cases, the spectral model of Justus and Paris (1985) was used for this study. For simulation of scenes with cloud cover, the model of Paris and Justus (1988) was used. These models have been recommended by the International Commission on Illumination (CIE, 1989) for the calculation of solar spectral irradiances.

Figure 3 shows results for sensor reflectance simulations for AVHRR channels 1 and 2, using the Justus and Paris model for the various surface spectral reflectances of Bowker et al. (including a variety of vegetation and soil types as well as water and snow surfaces). Clouds of a variety of optical depths were simulated with the Paris and Justus model. This figure shows the familiar "vegetation branch", in which vegetation is characterized by high values of sensor-band reflectance in channel 2 and low values of channel 1 reflectance.

The addition of channel 3A at 1.6 μm adds a third dimension to the simulated results, as shown in the two different perspective views of Figures 4 and 5. While the addition of this third dimension allows for a variety of analysis approaches, a popular and effective method is to use a form of principal component analysis know as the "tasseled cap" transform (Kauth and Thomas 1976; Crist and Cicone, 1984; Crist 1985; Crist and Kauth, 1986). The tasseled cap transform allows the three input values of reflectances in AVHRR channels 1, 2 and 3A (here measured in reflectance units) to be transformed into three empirically orthogonal parameters (similar in interpretation to eigenvectors of the covariance matrix of the reflectance data). The transformed variables are thus simple linear combinations of the input reflectances. Tasseled cap transform analysis of the data in Figures 4 and 5 yielded the following results for the transformed variables (B, G and D) from the original AVHRR sensor-band reflectances (CH1, CH2 and CH3A):

$$\begin{aligned} B &= 0.784\,CH1 + 0.556\,CH2 + 0.276\,CH3A \\ G &= -0.517\,CH1 + 0.831\,CH2 - 0.205\,CH3A \\ D &= -0.343\,CH1 + 0.018\,CH2 + 0.939\,CH3A. \end{aligned} \tag{1}$$

The transform variables B and G are conventionally labeled "Brightness" and "Greenness" because B corresponds approximately to the radial direction along the soil-cloud-snow branch of Figure 3, while G corresponds approximately to an orthogonal direction increasing along the vegetation branch of Figure 3. Figure 6 illustrates this property by plotting the CH1-CH2 data of Figure 3 after transformation and as seen in the B-G plane. The third tasseled cap transform variable (D), illustrated by the three dimensional plot of Figure 7, can be interpreted as "Dryness" (i.e. a parameter whose value increases as the moisture content decreases). Frequently a third tasseled cap parameter called "Wetness" is defined. If the coefficient values in the D component of equation (1) are reversed in sign, then such a "Wetness" parameter would result (i.e. Wetness values would increase as the moisture content increases).

Several of the surface spectral data sets of Bowker et al. (1985) consist of "wet-dry" pairs, that is spectral reflectance curves for the same surface type under conditions of high and low moisture content. These wet-dry pairs contain both vegetation and soil type representatives. That the tasseled cap transform parameters for the AVHRR reflectances represent a strong signal of both the vegetation moisture and the soil moisture content is illustrated by plotting the results for the Dryness versus Brightness (D-B) for the Bowker wet-dry pair data, as shown in Figure 8. In all cases, the dry member of the wet-dry pair is the one at the larger dryness value in Figure 8. The success of the AVHRR tasseled cap transform in measuring soil and vegetation moisture is not surprising in view of the fact that Landsat TM data (using all 7 TM bands) shows a good ability to measure soil moisture and vegetation moisture (Crist et al., 1986; Musick and Pelletier, 1988) through the use of tassseled cap transform variables.

We now examine the ability of the 3-channel AVHRR data to quantitatively estimate the soil moisture and vegetation moisture through the use of the tasseled cap transform variables. For this purpose we use observed soil moisture and vegetation moisture data from the First International Satellite Land Surface Climatology Project (ISLSCP) Field Experiment (FIFE). An overview of the FIFE project is provided by Sellers et al. (1992). The FIFE data are available in a 5-volume CD-ROM data set (Strebel et al., 1991). As a surrogate for the AVHRR with 1.6 μm, the FIFE Landsat imagery from Thematic Mapper band 3 (0.62-0.70 μm), band 4 (0.77-0.90 μm) and band 5 (1.6-1.8 μm) were used in place of AVHRR channels 1, 2 and 3A, respectively. The TM values (in reflectance units) were processed trough the AVHRR tasseled cap transform relations of equation (1) to yield Brightness (B), Greenness (G) and Dryness (D) parameters.

FIFE soil moisture data from either neutron probe or gravimetric technique (or an average of the two if both were available) were used from sites and times where simultaneous (same day) TM observations were available. Because of variability among the different soil types at the various sites, the Dryness values were not found to be uniquely related to soil moisture content. However, when data were examined with different soil moisture values observed at the same site on different days (each with a corresponding TM observation), then it was found that there is a close relationship between the observed changes in soil moisture content (in percent) and the change in

Dryness between the two days (in percent). The observed relationship is illustrated in Figure 9. The regression relation shown in Figure 9 is

$$\delta \text{ Soil Moisture } (\%) \quad = \quad 1.48 \quad - \quad 6.496 \ \delta \text{ Dryness}(\%) \tag{2}$$

This regression relation explains 68.9% of the original variance among the data points of Figure 9, with an rms residual error of 6.9% in the fitted values of soil moisture change.

Similarly, FIFE data on vegetation moisture were compared with observations of the TM-surrogate AVHRR Dryness parameter, as shown in Figure 10. The vegetation moisture content is expressed as a percent of dry vegetation weight. As a more relevant measure of the total amount of vegetation moisture in the satellite scene, the vegetation moisture values are multiplied by the measured values of leaf-area-index (LAI). Figure 10 shows good correspondence between LAI × Vegetation Moisture and tasseled cap Dryness parameter. The regression

$$\text{LAI} \times \text{Vegetation Moisture } (\%) \quad = \quad 376.4 \quad - \quad 17.46 \text{ Dryness } (\%) \tag{3}$$

explains 79.4% of the original variance in the data points of Figure 10, with a residual error of 21.6% in the fitted values of LAI × Vegetation Moisture.

Discussion and Recommendations

The spectral model results of Figure 8 and the FIFE observational data using TM-surrogate data for AVHRR with the 1.6 μm channel 3A, indicate that the tasseled cap transform variables using AVHRR reflectance data will be very effective in the quantitative measurement of soil moisture and vegetation moisture. Since the AVHRR data have nominal 1 km resolution (LAC data) or 4 km resolution (GAC data), these soil moisture and vegetation moisture observations with AVHRR will serve as useful adjuncts to be used in combination with soil moisture or vegetation moisture derived from (perhaps more accurate, but lower spatial resolution) microwave sensors.

Recently, Nemani et al. (1993) have shown that there is value in combining AVHRR-derived surface temperature measurements with normalized vegetation index values to estimate soil moisture. Improvements over the use of AVHRR tasseled cap Dryness parameter alone are also likely with the addition of satellite-derived surface temperature information. The FIFE data would also provide a good set of observations (Jedlovec and Atkinson, 1992) against which to test this hypothesis.

Figures 6 and 7 show that the AVHRR tasseled cap transform variables are also useful in discriminating snow and clouds, and in distinguishing vegetation from soils. The tasseled cap transform variables, forming an empirical orthogonal set as they do, tend to maximize the variance (and minimize the covariance) among the transformed data values. This feature should lead to improved discrimination among all types of phenomena. Hence, the AVHRR tasseled cap transform parameters of Brightness, Greenness and Dryness, as provided by equation (1), should also be useful in distinguishing water-phase clouds from ice-phase clouds, in determining the presence and optical properties of cirrus clouds and in providing additional optical information about atmospheric aerosols.

References

Bowker, D. E. et al. (1985): Spectral Reflectances of Natural Targets for Use in Remote Sensing Studies", NASA Reference Publication 1139, June.

CIE (1989): "Solar Spectral Irradiance", Technical Committee 2-17 of the International Commission on Illumination, CIE Publ. No. 85 (ISBN 3 900 734 22 4).

Crist, E.P. (1985): "A TM Tasseled Cap Equivalent Transformation for Reflectance Factor Data", **Remote Sensing of Environment, 17**, 301-306.

Crist, E.P and R.C. Cicone (1984): "Application of the Tasseled Cap Concept to Simulated Thematic Mapper Data", **Photogrammetric Engineering and Remote Sensing, 50**(3), 343-352.

Crist, E.P. and R.J. Kauth (1986): "The Tasseled Cap De-Mystified", **Photogrammetric Engineering and Remote Sensing, 52**(1), 81-86.

Crist, E.P. et al. (1986): "Vegetation and Soils Information Contained in Transformed Thematic Mapper Data", Proc. Int. Geoscience and Remote Sensing Symp., 1465-1470.

Ehrlich, D., J.E. Estes and J. Seepan (1993): "Crop Monitoring in Italy", **ERDAS Monitor**, **5**(2), 1-8.

Jedlovec, G.J. and R.J. Atkinson (1992): "Variability of Geophysical Parameters from Aircraft Radiance Measurements for FIFE", **J. Geophys. Res., 97**(D17), 18913-18,924.

Justus, C.G. and M.V. Paris (1985): "A Model for Solar Spectral Irradiance and Radiance at the Bottom and Top of a Cloudless Atmosphere", **J. Climate Appl. Meteorol., 24**, 193-205.

Justus, C.G. and M.V. Paris (1987): "Sensitivity of Proposed New AVHRR Channel Filters to Aerosols, Water Vapor and Viewing Angle Factors", Proc. 2nd Cof. Satellite Meteorology/Remote Sensing and Applications, May 13-16, Williamsburg, VA, pp.259-262.

Kauth, R.J. and G.S. Thomas (1976): "The Tasseled Cap - A Graphic Description of the Spectral-Temporal Development of Agricultural Crops as seen by Landsat", Proc. Symp. Machine Processing of Remotely Sensed Data, 4B-41 - 4B-51.

Masuda, K. and T. Takashima (1990): "Deriving Cirrus Information using the Visible and near-IR Channels of the Future NOAA-AVHRR Radiometer", **Remote Sensing of Environment, 31**(1), 65-81.

Musick, H.B. and R.E. Pelletier (1988): "Response to Soil Moisture of Spectral Indexes Derived from Bidirectional Reflectance in Thematic Mapper Wavebands", **Remote Sensing of Environment, 25**, 167-184.

Nemani, R., L. Pierce, S. Running and S. Goward (1993): "Developing Satellite-derived Estimates of Surface Moisture Status", **J. Appl. Meteorol., 32**(3), 548-557.

Paris, M.V. and C.G. Justus (1988): "A Cloudy-Sky Radiative Transfer Model Suitable for Calibration of Satellite Sensors:, **Remote Sensing of Environment, 24**(2), 269-285.

Pereira, M.C. and A.W Setzer (1993): "Spectral Characteristics of Fire Scars in Landsat-TM Images of Amazonia", **Int. J. Remote Sensing, 14**(11), 2061-2078.

Perry, C.R. and L.F. Lautenschlager (1984): "Functional Equivalence of Spectral Vegetation Indices", **Remote Sensing of Environment, 14**, 169-182.

Pilewskie, P. and S. Twomey (1986): "Cloud Spectral Reflectance in the Near-Infrared", 6th Conf. on Atmospheric Radiation, Williamsburg, VA.

Sellers, P.J. et al. (1992): "An Overview of the First International Satellite Land Surface Climatology Project (ISLSCP) Field Experiment (FIFE)", **J. Geophys. Res., 97**(D17), 18,345-18,371.

Strebel, D.E. et al. (1991): "Collected Data of the First ISLSCP Field Experiment", published on CD-ROM by NASA.

Townsend, J. et al. (1991): "Global Land Cover Classification by Remote Sensing: Present Capabilities and Future Possibilities", **Remote Sensing of Environment, 35**, 243-255.

Tucker, C.J. (1978): "A Comparison of Satellite Sensor Bands for Vegetation Monitoring", **Photogrammetric Engineering and Remote Sensing, 44**(11), 1369-1380.

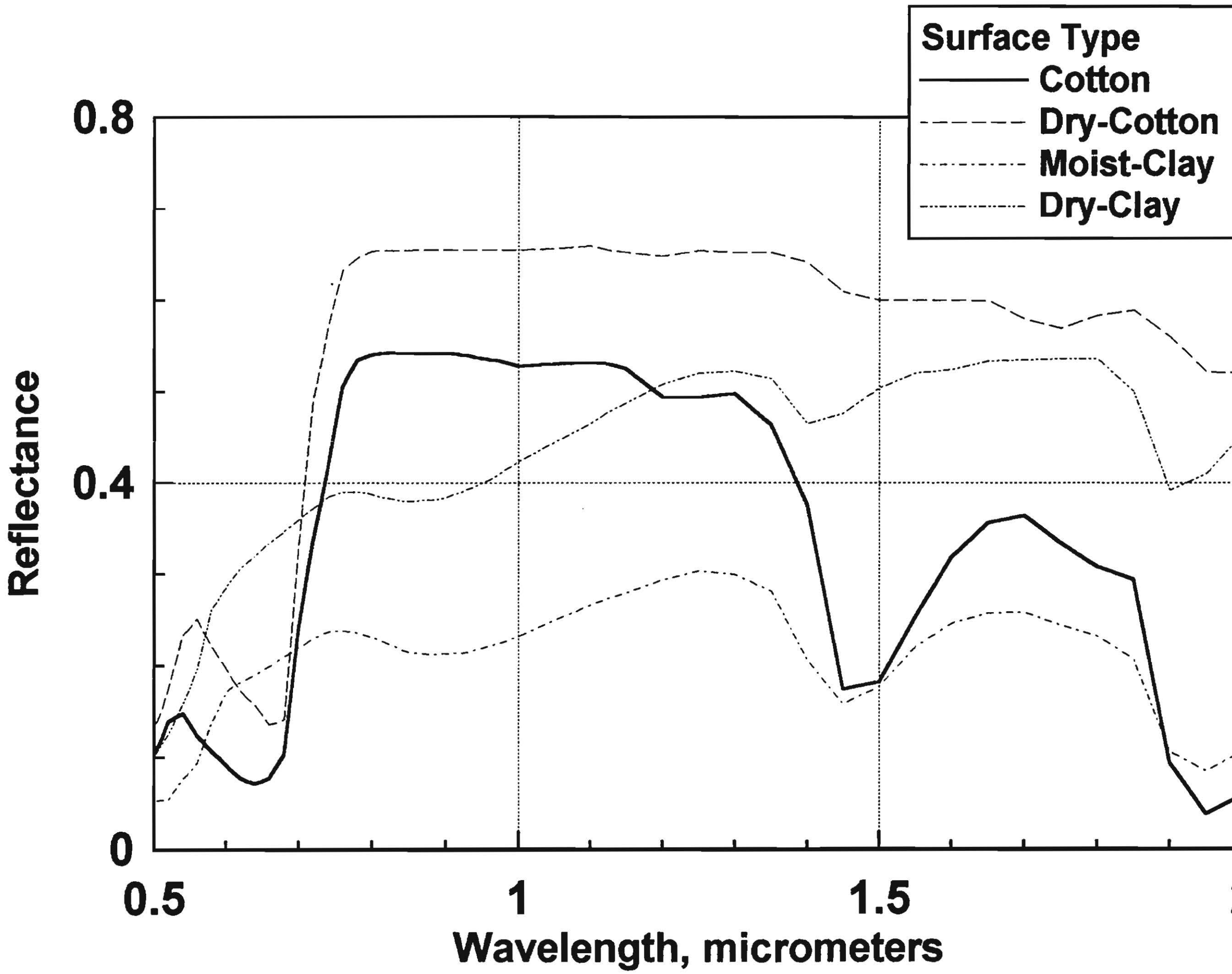

Figure 1 - Spectral reflectance curves (Bowker et al., 1985) for moist and dry cotton and moist and dry clay.

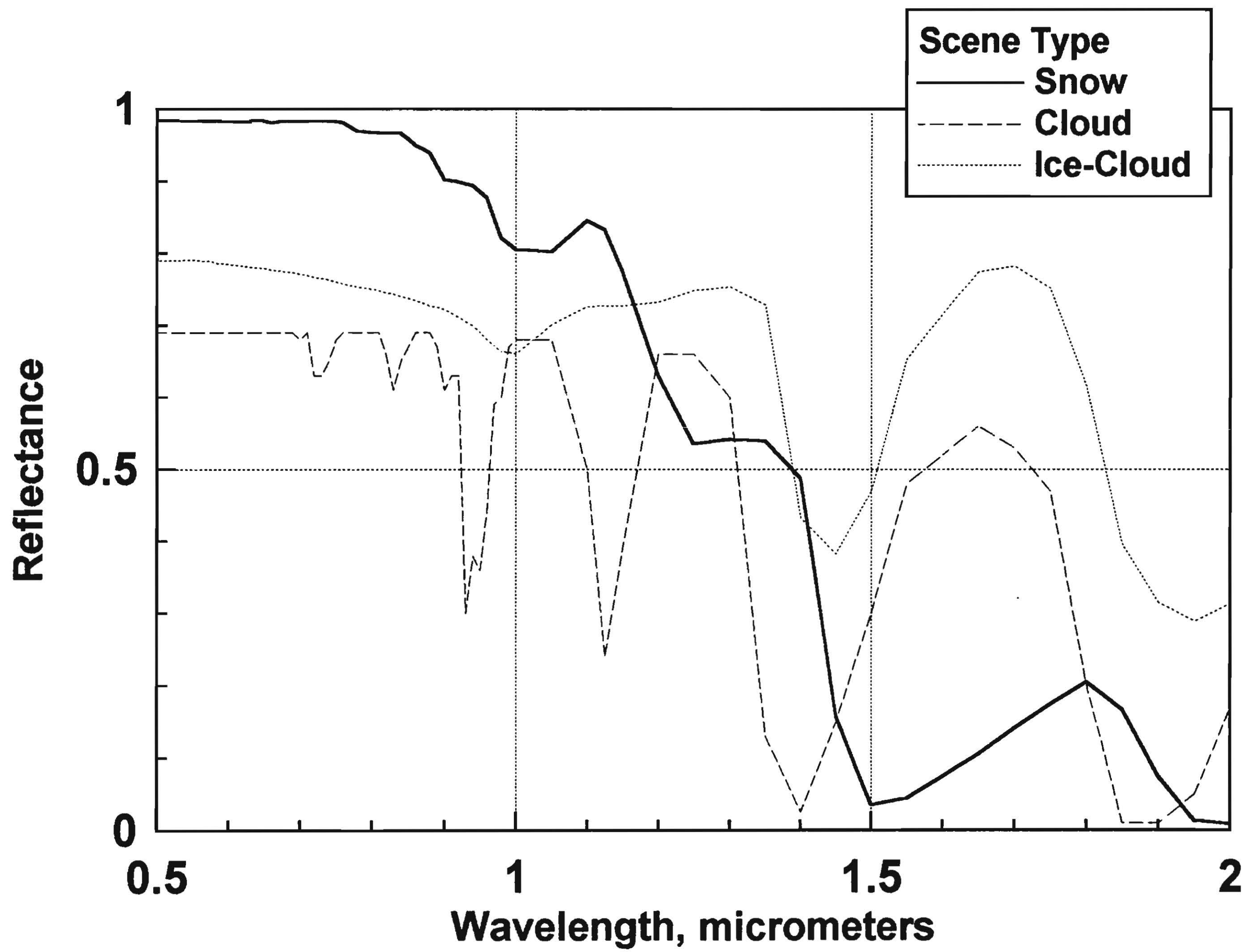

Figure 2 - Spectral reflectance curves (Bowker et al., 1985) for fresh snow, water-phase cloud and ice-phase cloud.

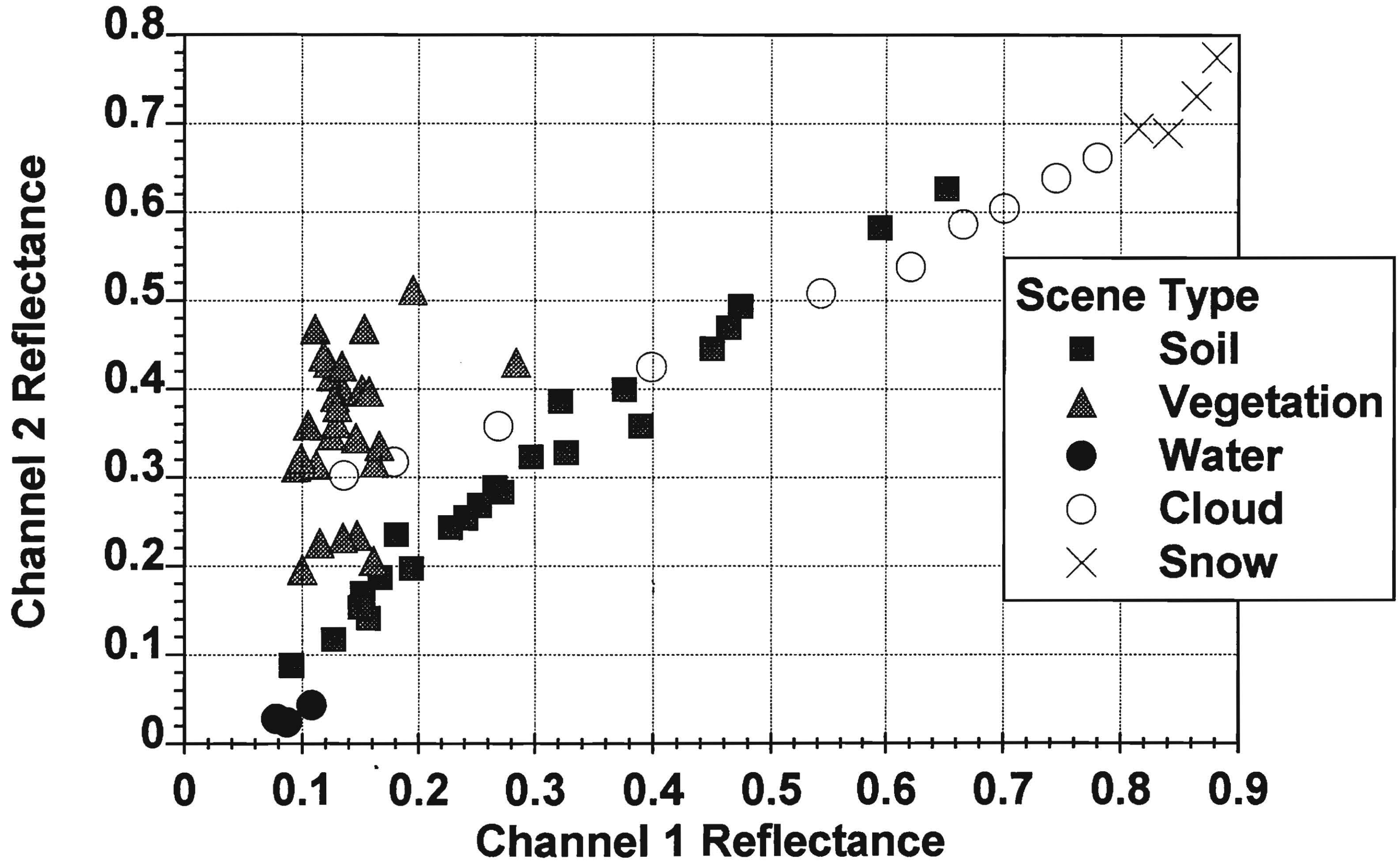

Figure 3 - Simulated AVHRR sensor-band reflectances for a variety of surface reflectances and cloud optical depths.

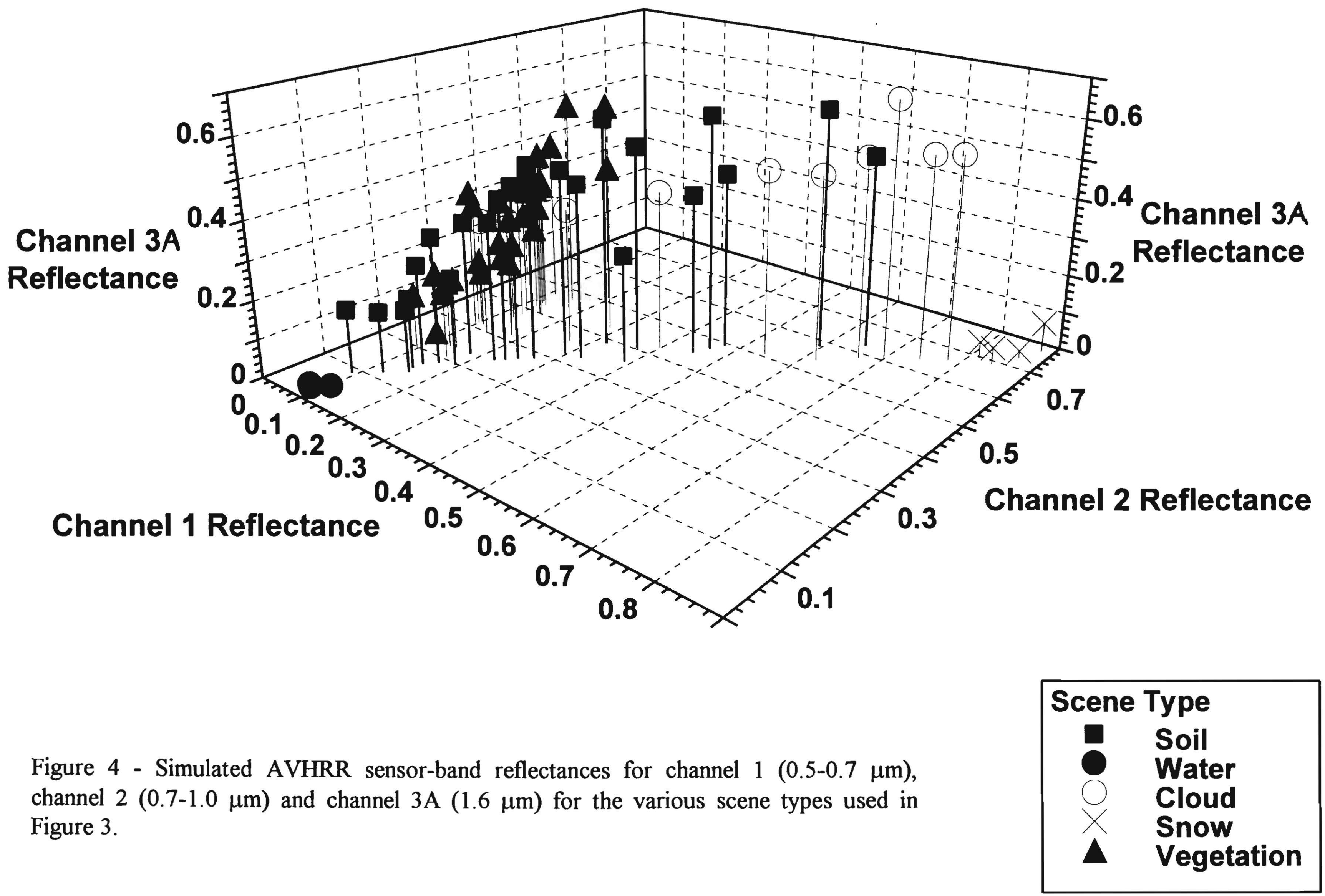

Figure 4 - Simulated AVHRR sensor-band reflectances for channel 1 (0.5-0.7 μm), channel 2 (0.7-1.0 μm) and channel 3A (1.6 μm) for the various scene types used in Figure 3.

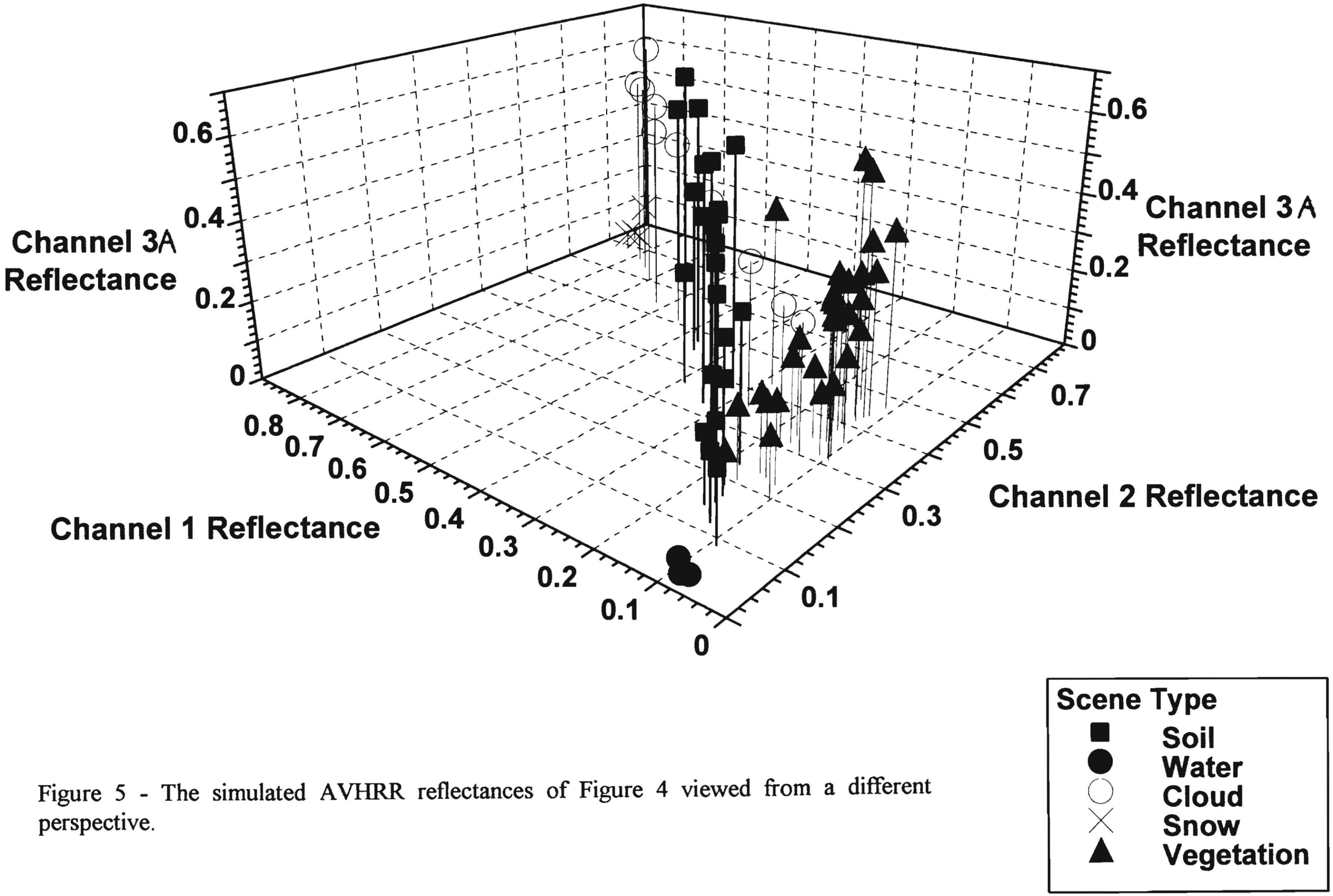

Figure 5 - The simulated AVHRR reflectances of Figure 4 viewed from a different perspective.

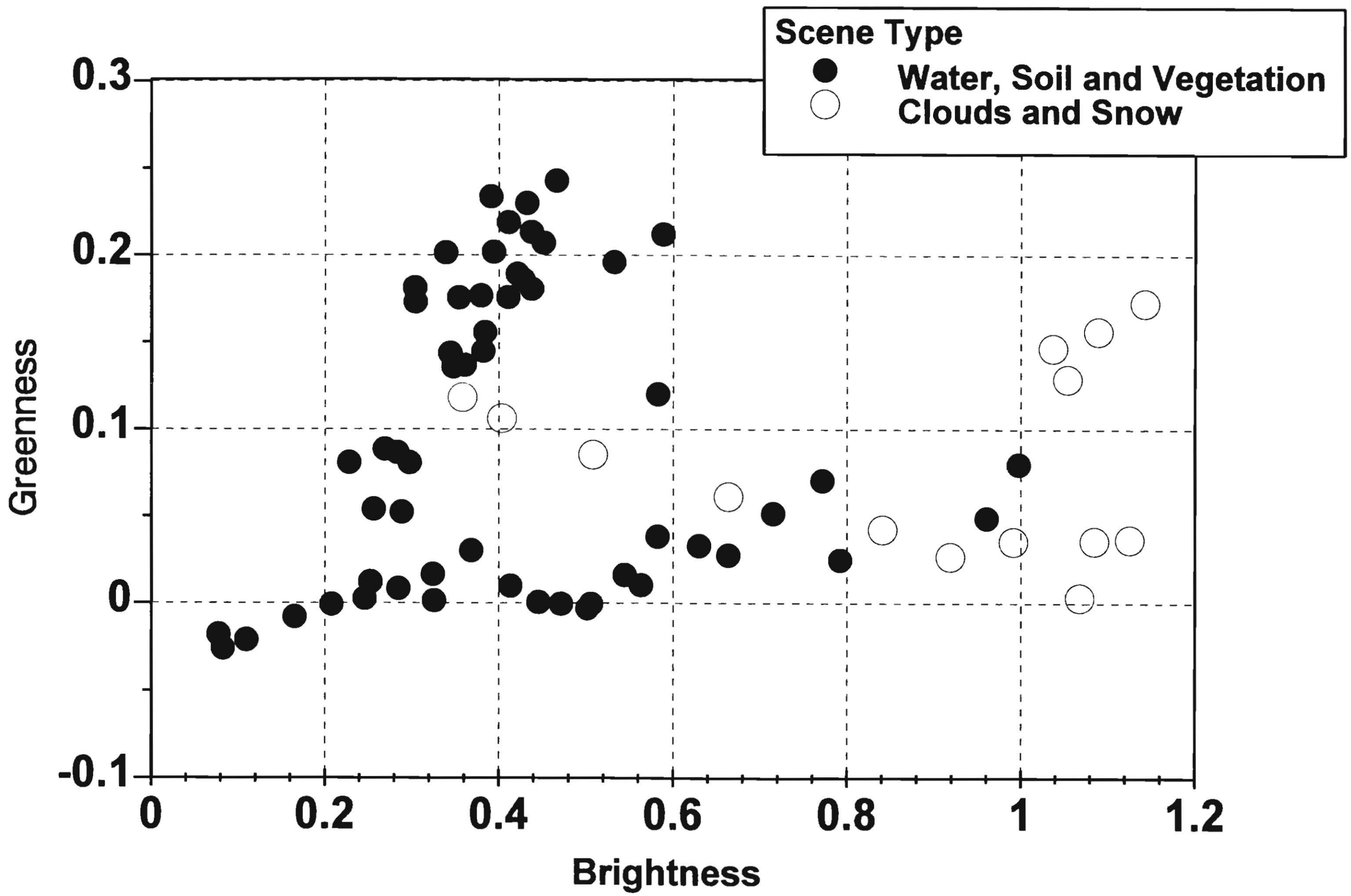

Figure 6 - The Brightness-Greenness (B-G) plane of the tasseled cap transform data from Figure 3.

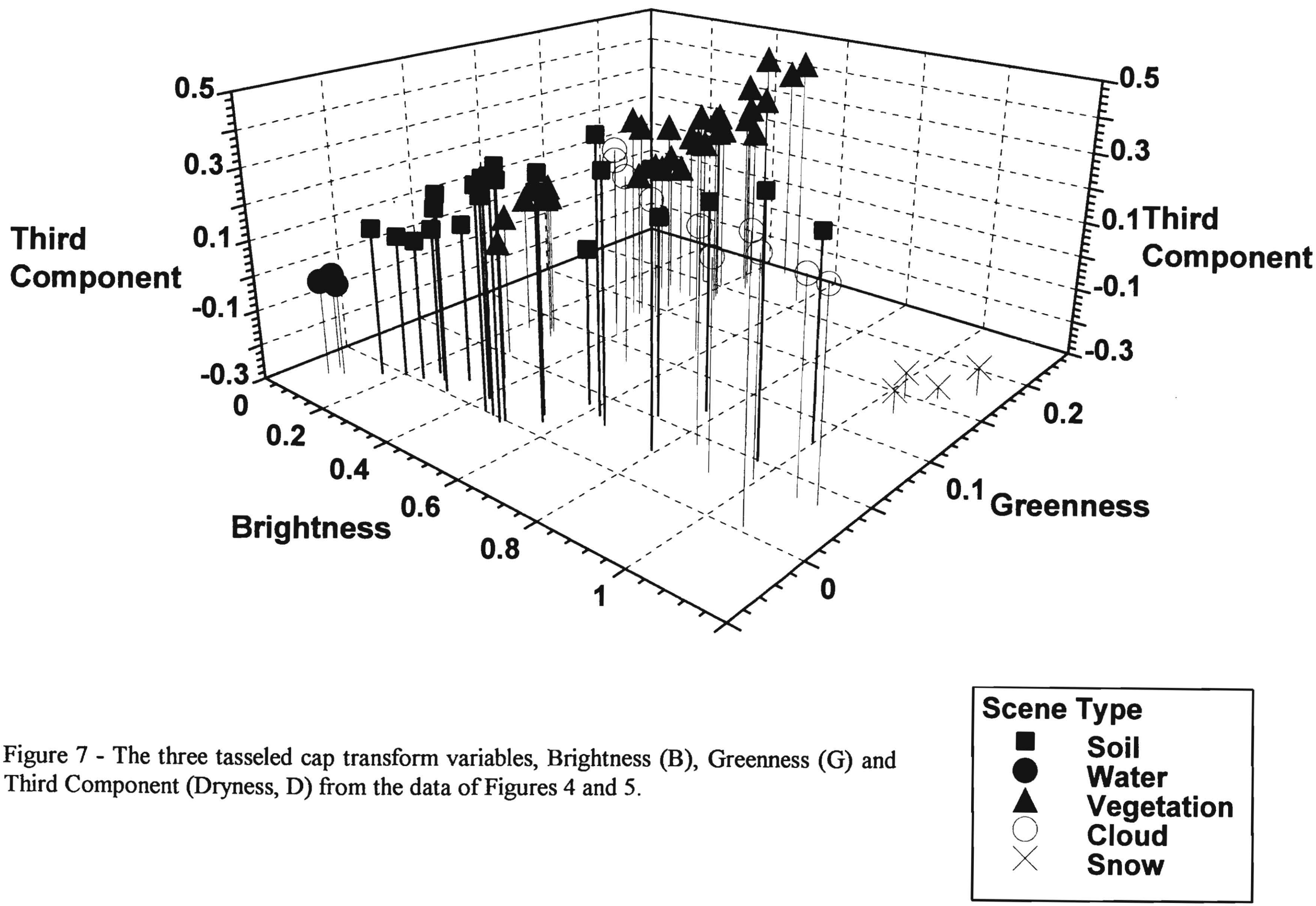

Figure 7 - The three tasseled cap transform variables, Brightness (B), Greenness (G) and Third Component (Dryness, D) from the data of Figures 4 and 5.

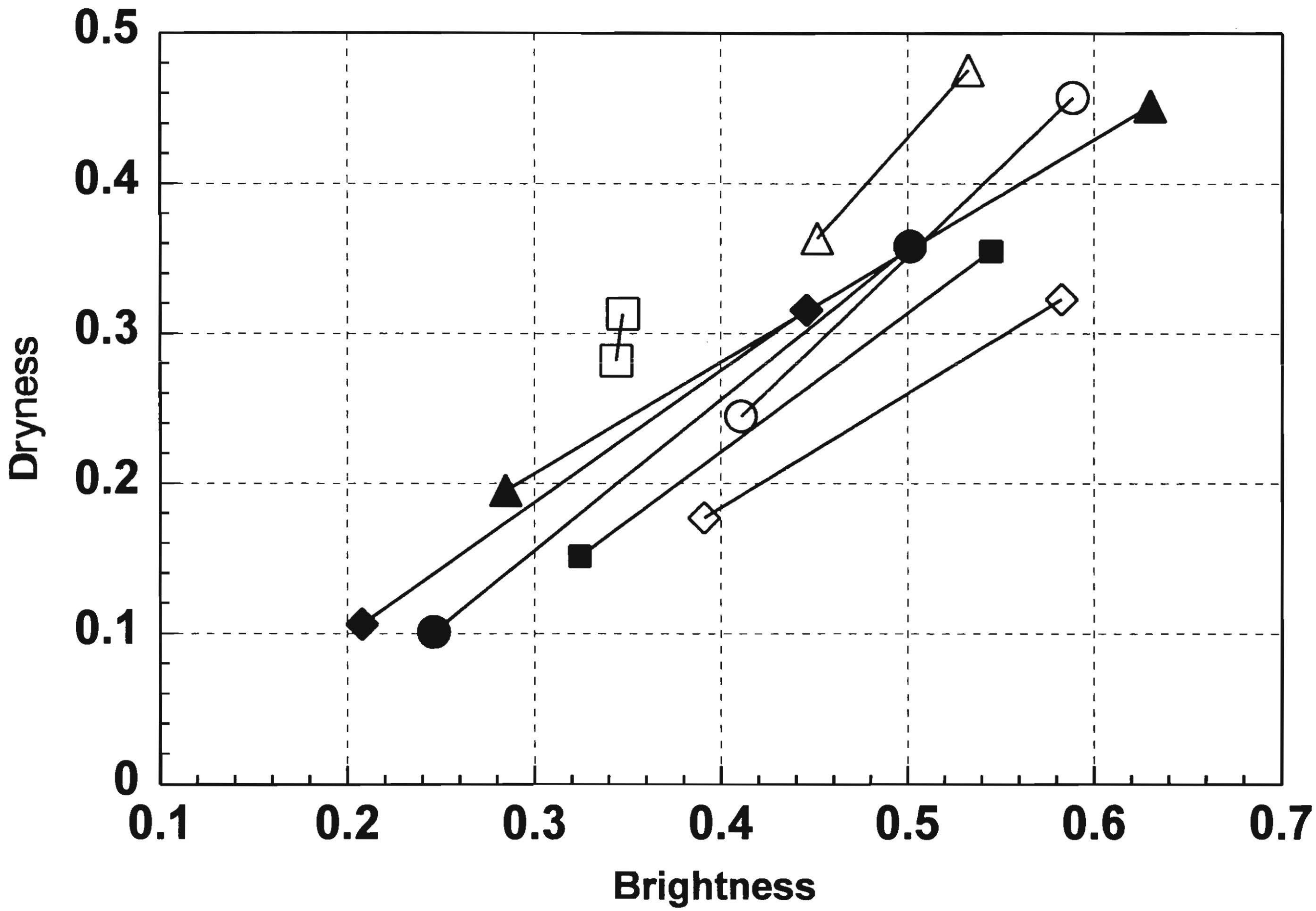

Figure 8 - Dryness versus Brightness (D-B) for various wet and dry soil types (open symbols) and vegetation types (solid symbols) from the Bowker et al. (1985) spectral reflectances: □ = clay, ❍ = clay soil, ◊ = sandy soil, Δ = silt, ■ = beans, • = cotton, ♦ = pine, ▲ = sycamore.

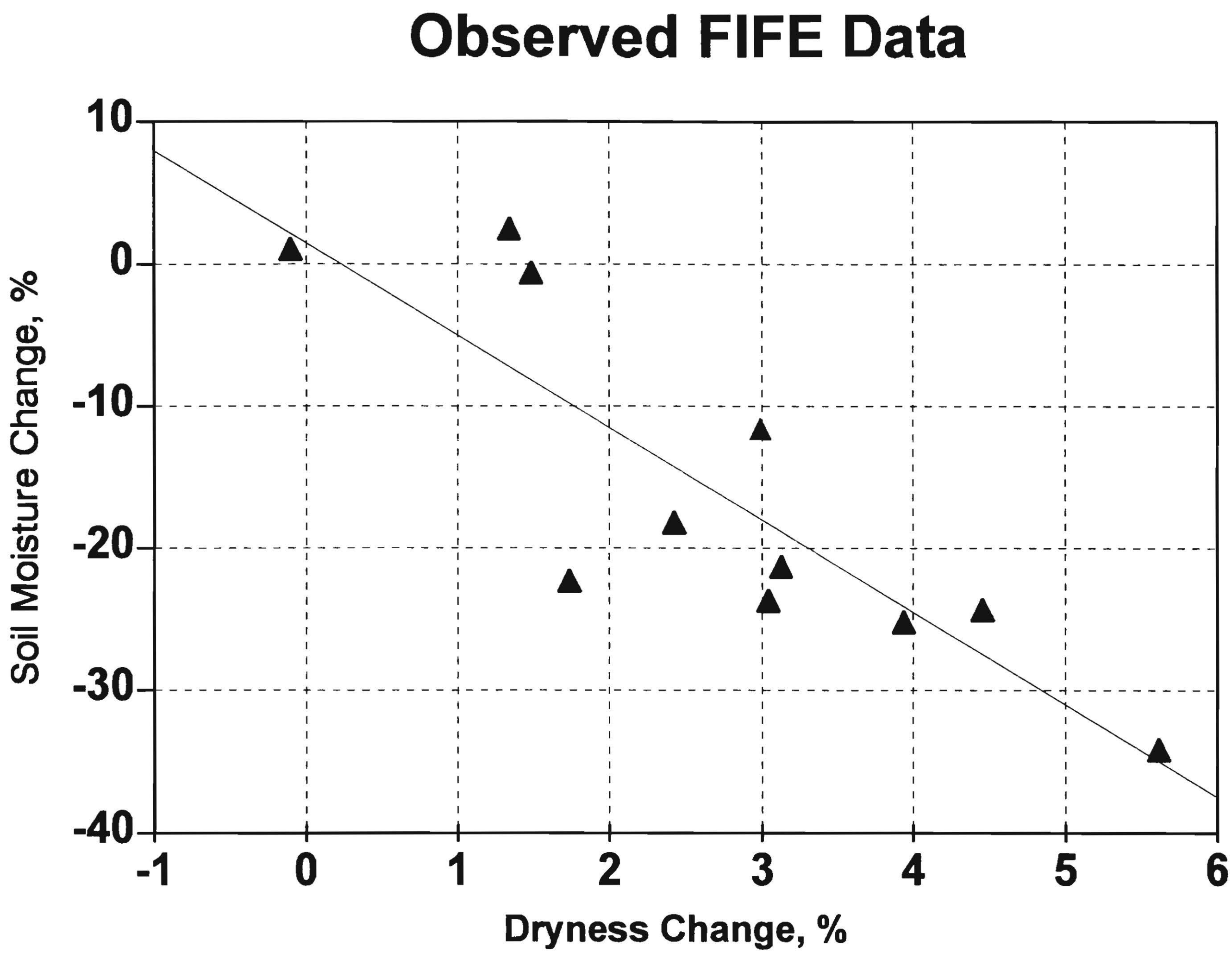

Figure 9 - Observed FIFE soil moisture change between observations versus observed TM-surrogate AVHRR Dryness value change between observations.

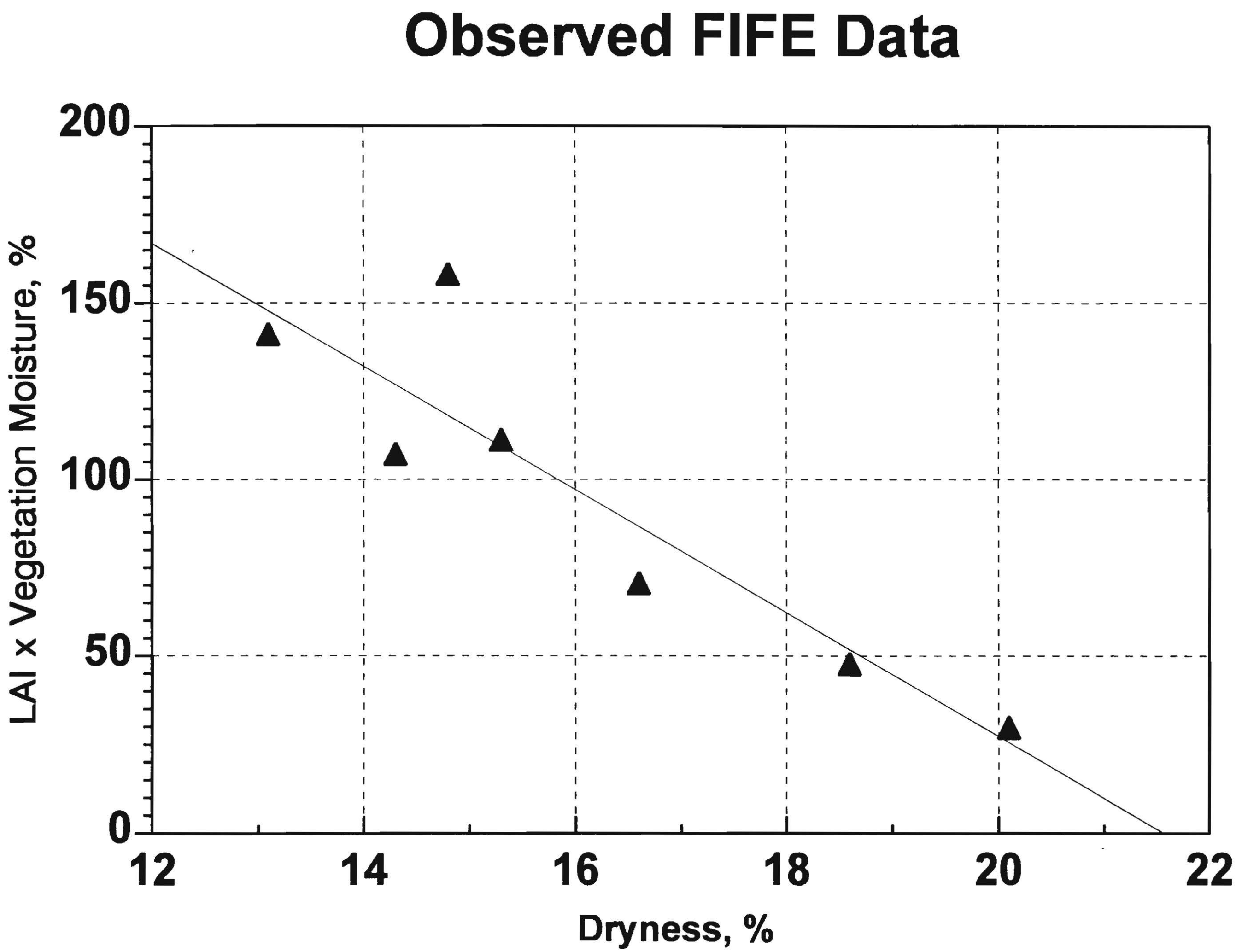

Figure 10 - Observed FIFE data for the product of vegetation moisture (% dry weight) times leaf-area-index (LAI) versus the observed TM-surrogate AVHRR Dryness parameter.